Journal of Magnetic Resonance 193 (2008) 150–152

Contents lists available at ScienceDirect

Journal of Magnetic Resonance

journal homepage: www.elsevier.com/locate/jmr

Communication

# The generation of intense radiofrequency fields in μcoils

Edward W. Hagaman [a,*], Jian Jiao [a], Tony Moore [b]

[a] Chemical Sciences Division, Oak Ridge National Laboratory, P.O. Box 2008, 1 Bethel Valley Road, Oak Ridge, TN 37831-6201, USA
[b] Engineering Science & Technology Division, Oak Ridge National Laboratory, Oak Ridge, TN 37831, USA

ARTICLE INFO

*Article history:*
Received 27 February 2008
Revised 4 April 2008
Available online 1 May 2008

*Keywords:*
μCoil probe
Radiofrequency (rf) field
$^{19}$F NMR
μCoil probe construction

ABSTRACT

Large amplitude radiofrequency (rf) fields hold great promise in wide line NMR where it becomes possible to excite the full breadth of the line in a quantitative fashion. Applications in quadrupole NMR and in NMR of paramagnetic systems benefit greatly from intense fields. Spin manipulations in multiple quantum NMR experiments, specifically, the generation of multiple quantum coherence in MQ NMR, are more efficiently produced using intense rf fields. In this work we describe a μcoil probe that produces an rf field of 25 MHz, more than five times larger than the greatest rf field reported in the literature. We accomplish this in a robust, 127 μm diameter solenoid coil using 1 kW of rf power.



## 1. Introduction

The use of microcoils (μcoils) for NMR analysis of dissolved, mass limited solutes has been actively pursued for more than a decade [1–6] and applications of μcoil techniques for static solid state NMR studies have appeared in the last few years [7–9]. Very recently μcoil NMR has been implemented in MAS probeheads for applications to solids [10,11]. Large radiofrequency (rf) fields are beneficial in solid state NMR to uniformly excite broad (MHz) resonances, as in quadrupole NMR or in NMR studies of paramagnetic materials. Large rf fields improve efficiency in the population of multiple quantum (MQ) manifolds and so enhance signal-to-noise in MQ NMR experiments [12]. In this work a μcoil probe is described that generates rf fields of 25 MHz, more than five times larger than the greatest rf field reported in the literature. These fields are produced in a robust, 127 μm diameter solenoid coil using 1 kW of rf power [13].

## 2. Experimental

The μcoil probe uses a jig-wound copper solenoid coil. The physical L/C circuit design is after that of van Bentum et al. [8], a clever arrangement that minimizes lead lengths and associated inductive losses by mounting the coil in the body of the circuit capacitor. A cartoon of the L/C circuit is shown in Fig. 1. A photograph of the probehead and the circuit diagram are shown in Fig. 2.

The coil is wound on a glass capillary drawn from 1.5 mm capillary (VWR 50 μL microdispenser, Catalog No. 53508-466). Fine capillaries with 30–150 μm outer diameters can be made by hand-drawing the capillary over a Bunsen burner flame. The coil is made from 25 μm copper wire coated with a polyurethane insulation layer and polyvinyl butyral overcoat (50 P Bond #1, MWS Wire Industries, Westlake Village, CA) for a finished wire diameter of 32 μm. The coil is close-wound on a hand-turned jig producing a near-optimum wire-diameter-to-wire-spacing ratio, $d/s = 0.8$ [14]. The butyral coating is a thermoset polymer that melts at 125 °C. The coil and jig assembly are oven-heated to 130 °C and held at this temperature for 5 min to unitize the coil capillary assembly. After cooling, the coil is rugged enough to remove from the jig and mount in the capacitor.

The capacitor was made from a 25.4 mm diameter, 500 μm thick fused quartz disc (University Wafers, Boston, MA). The relative dielectric constant, $\xi_r$, for this material is 3.75. The disc surfaces are metallized with copper tape, trimmed to fit. The calculated capacity, $(\xi_0 \xi_r \pi r^2)$/thickness, is 33.1 pF, about 14% larger than the measured value, 29 pF. The operating voltage is limited by breakdown in air around the edge of the capacitor.

A 200 μm diameter hole is drilled through the capacitor center, normal to the surface plates (0.2 mm carbide tipped drill bit, Part No. 108911, available from LPKF Laser and Electronics, NA, Wilsonville, OR). The coil/capillary assembly is inserted in this hole, centered on its long axis between the capacitor plates, and glued into place using a drop of 5-min epoxy. After mounting, the capillary tube is cut-off several mm above and below the capacitor plate surfaces. The coil leads are soldered to the capacitor plates with care to minimize the lead lengths. This L/C device (Fig. 1), the heart of the probe, is mounted on a probehead with the coil axis perpendicular to $H_0$ and connected to the rf source through a subminiature version A (SMA) rf connector soldered to the edge of the capacitor.

* Corresponding author. Fax: +1 865 574 6721.
*E-mail address:* hagamanew@ornl.gov (E.W. Hagaman).

1090-7807/$ - see front matter © 2008 Elsevier Inc. All rights reserved.
doi:10.1016/j.jmr.2008.04.022

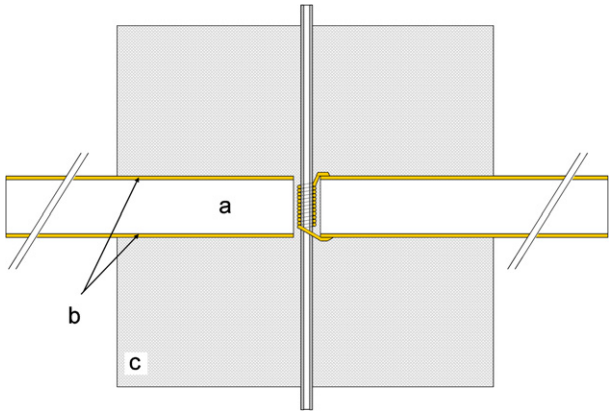


**Fig. 1.** Cartoon of the L/C geometry. The 13 turn coil ($l$ = 416 μm) is embedded in the copper-clad capacitor dielectric (a) (500 μm thick, 25.4 mm diameter). Coil leads are soldered to the copper capacitor plates (b) and the coil/capillary assembly is held in place with epoxy (c). The capillary extends above the epoxy and ends in a sample reservoir.

The capillary tube extensions on both capacitor faces are enclosed by an internally threaded fitting (Nanoport assembly N-123S, Upchurch Scientific, Oak Harbor, WA) that is glued to the plate surfaces. The fitting forms an annulus around the capillary that is filled with epoxy. The glue provides strength for the capillary extensions and a physical barrier that prevents solvent/solutes access to the coil volume except via the capillary tube. The Nanoport assembly is the transition to a flexible 510 μm o.d./125 μm i.d. polyetheretherketone (PEEK) capillary tube used to draw liquid samples into the probe by vacuum (Fig. 2).

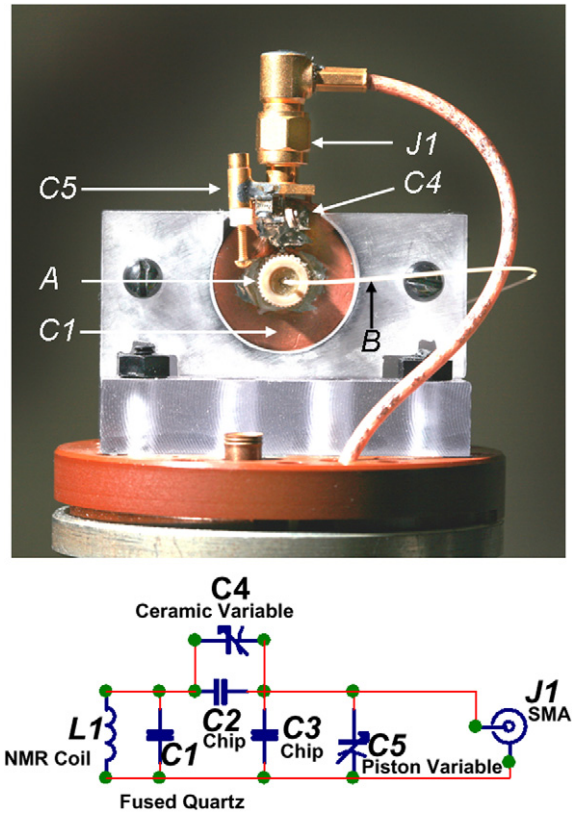


**Fig. 2.** (Top) Photograph of the probehead. *A* and *B* point to plumbing parts, the Nanoport assembly and the PEEK capillary tube, respectively. (Bottom) Circuit diagram of the probe. Several of the components are identified in the photo.

The coil used in this work has the following physical dimensions: diameter = 127 μm; turns = 13; length = 416 μm; length of wire in coil = 5.2 mm. Calculated electrical properties are $L$ = 5.42 nH; reactance = 12.88 Ω; resistance(ac) = 1.21 Ω; unloaded $Q$ (calculated) = 11 [15]. The $Q$ for the L/C circuit was measured from the impedance/frequency curve for parallel resonant circuits and is given by the ratio of the resonance frequency to the width of the resonance curve at the 6 dB point: 376.5/34.5 = 10.9 [16].

The coil is tuned to 376.5 MHz, the $^{19}$F Larmor frequency at 9.4 T, by adjusting the number of turns of the coil. Fine tuning and matching are accomplished by feeding the rf to the center of a tapped capacitor network mounted on the SMA connector and wired in parallel with the fused quartz capacitor. Hexafluorobenzene, HFB, as the neat liquid, is used for all measurements in this work. With our commercial solution probe the $^{19}$F resonance of HFB is a symmetrical Lorentzian line with $\nu_{1/2}$ = 2 Hz. In the μcoil probe the HFB resonance presents a highly asymmetric line with a shape expected for the magnetic susceptibility perturbation due to a thin-walled cylinder, a reasonable approximation for the close-wound μcoil [17]. The full width of the resonance is 2 ppm (750 Hz). No susceptibility matching techniques were implemented on this probe. The line shape was insensitive to shimming with the room temperature shims. In the nutation experiments described below extreme parts of the asymmetric lineshape follow similar nutation curves, yielding π/2 pulse times which differ by less than 50%. We conclude that the dominant signal derives from

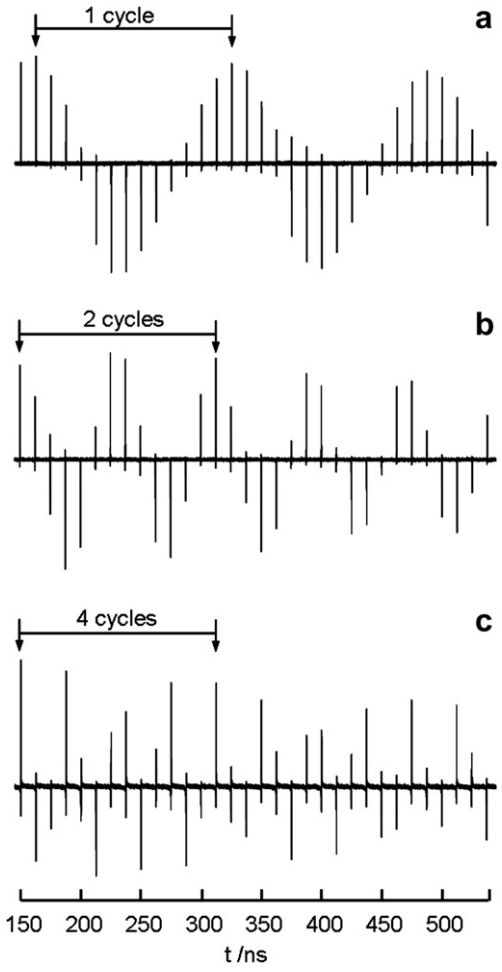


**Fig. 3.** Nutation plots of the $^{19}$F resonance of hexafluorobenzene: the time interval indicated by the arrows is 162.5 ns. The amplitude of the rf field, the inverse of the period, is 6.2, 12.4, and 24.8 MHz, in (a), (b), and (c), respectively.

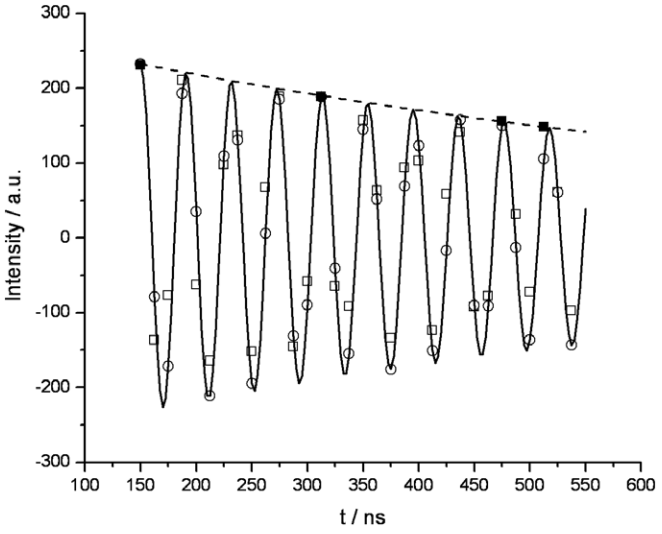


**Fig. 4.** The signal intensity data from Fig. 3c fit as decaying cosine function, $I = Aexp(-t/T_2^*)\cos(\omega t)$. $T_2^*$, evaluated from the solid experimental points in the figure that define the envelope decay (■) is 800 ns, experimental data: □, model points: ○. The period is 40.6 ns; the rf field strength is 24.6 MHz.

the sample in the coil volume and that this signal shows a strong magnetic susceptibility broadening. Signal broadening of this extent is a major concern for solution state studies but will be of little consequence in many solid state NMR applications.

## 3. Results and discussion

Fig. 3 presents nutation plots of the $^{19}F$ resonance of HFB measured on the μcoil probe. Individual spectra were acquired in eight scans using single pulse excitation and a 1 s pulse repetition rate. The pulse length is incremented in the minimum time interval of the spectrometer, 12.5 ns. The data are displayed over an arbitrary time interval and an initial pulse length of 150 ns. The sample is not restricted to the coil volume. The capillary-constrained liquid sample extends along the coil axis 4–6 coil lengths beyond the coil ends and then opens to a solvent/sample reservoir.

At low power levels (56 W) the rf field in the coil is 6.2 MHz, corresponding to a 41 ns 90° pulse (Fig. 3a). A fourfold increase in power doubles the rf field amplitude to 12.4 MHz (20 ns 90° pulse, Fig. 3b). The power level used in this experiment, 256 W, is typical of that used in conventional solid state NMR probes. Our commercial broadband HX double-tuned 4 mm solids probe, for example, produces an rf field amplitude of 195 kHz (1.3 μs 90° pulse) with 256 W pulse power. Rf field amplitude scales with the inverse of the coil diameter for solenoid coils with constant l/*d* ratio [8]. The μcoil probe of van Bentum et al. uses a solenoid coil geometry similar to ours [8]. These authors generate an rf field of 4.7 MHz in a 350 μm coil with 270 W. At this power the expected field in a coil with $d = 127$ μm, the diameter of our coil, is 13.0 MHz. This value is comparable to the 12.4 MHz rf field we measure in our probe using 256 W.

The nutation plot generated by nearly quadrupling the power again is shown in Fig. 3c. Approximately 1 kW of power applied to the probe in this series demonstrates the ruggedness of the μcoil circuit design. The 90° pulse estimated from inspection of this plot is 10 ns, less than the minimum time interval of the spectrometer! The field amplitude was determined with better precision by fitting the signal intensity to a decaying cosine function (Fig. 4). The oscillation period, 40.6 ns, corresponds to a 24.6 MHz rf field amplitude.

## 4. Conclusion

Intense, 25 MHz rf fields have been generated in a robust μcoil probe. A direct, though mechanically tedious, extension of this work, reducing the coil diameter a factor of two or three, will allow the generation of rf fields in excess of 50 MHz [18]. We anticipate that μcoil probes will find extensive application in wide line NMR studies.

## Acknowledgments

Research sponsored by the Laboratory Directed Research and Development Program of Oak Ridge National Laboratory (ORNL), managed by UT-Battelle, LLC for the U.S. Department of Energy, and in part by the Division of Chemical Sciences, Geosciences, and Biosciences, Office of Basic Energy Sciences, U.S. Department of Energy under contract DE-AC05-00OR22725 with Oak Ridge National Laboratory, managed and operated by UT-Battelle, LLC.

## References

[1] D.L. Olsen, T.L. Peck, A.G. Webb, R.L. Magin, J.V. Sweedler, High-resolution microcoil $^1H$ NMR for mass-limited nanoliter-volume samples, Science 270 (1995) 1967–1970.
[2] R. Subramanian, A.G. Webb, Design of solenoidal microcoils for high resolution $^{13}C$ NMR spectroscopy, Anal. Chem. 70 (1998) 2454–2458.
[3] D.L. Olsen, M.E. Lacey, J.V. Sweedler, High-resolution microcoil nmr for analysis of mass-limited nanoliter samples, Anal. Chem. 70 (1998) 645–650.
[4] S.C. Grant, N.R. Aiken, H.D. Plant, S. Gibbs, T.H. Mareci, A.G. Webb, S.J. Blackband, NMR spectroscopy of single neurons, Magn. Reson. Med. 44 (2000) 19–22.
[5] K.R. Minard, R.A. Wind, Picoliter $^1H$ NMR spectroscopy, J. Magn. Reson. 154 (2002) 336–343.
[6] Y. Maguire, I.L. Chuang, S. Zhang, N. Gershenfeld, Ultra-small-sample molecular structure detection using microslot waveguide nuclear spin resonance, Proc. Natl. Acad. Sci. USA 104 (2007) 9198–9203.
[7] K. Yamauchi, J.W.G. Janssen, A.P.M. Kentgens, Implementing solenoid microcoils for wide-line solid-state NMR, J. Magn. Reson. 167 (2004) 87–96.
[8] P.J.M. van Bentum, J.W.G. Janssen, A.P.M. Kentgens, Towards nuclear magnetic resonance μ-spectroscopy and μ-imaging, Analyst 129 (2004) 793–803.
[9] K. Yamauchi, T. Imada, T. Asakura, Use of microcoil probehead for determination of the structure of oriented silk fibers by solid-state NMR, J. Phys. Chem. B 109 (2005) 17689–17692.
[10] H. Janssen, A. Brinkmann, E.R. van Eck, P.J. Van Bentum, A.P.M. Kentgens, Microcoil high resolution magic angle spinning NMR spectroscopy, J. Am. Chem. Soc. 128 (2006) 8722–8723.
[11] D. Sakellariou, G. Le Goff, J.-F. Jacquinot, High-resolution, high-sensitivity NMR of nanolitre anisotropic samples by coil spinning, Nature 447 (2007) 694–697.
[12] J.-P. Amoureux, M. Pruski, D.P. Lang, C. Fernadez, The effect of RF power and spinning speed on MQMAS NMR, J. Magn. Reson. 131 (1998) 170–175.
[13] E.W. Hagaman, Jian Jiao, Tony Moore, NMR on small samples: the generation of intense radiofrequency fields in μcoils, Presentation at the 49th Rocky Mountain Conference on Analytical Chemistry, Brekenridge, CO, July 22–26, 2007.
[14] D.A. Seeber, R.L. Cooper, L. Ciobanu, C.H. Pennington, Design and testing of high sensitivity microreceiver coil apparatus for nuclear magnetic resonance and imaging, Rev. Sci. Instrum. 72 (2001) 2171–2179.
[15] H.A. Wheeler, Simple inductance formulas for radio coils, Proc. IRE 16 (1928) 1398.
[16] F.E. Terman, Radio Engineers' Handbook, McGraw-Hill, New York, 1943. p. 145.
[17] L.F. Fuks, F.S.C. Huang, C.M. Carter, W.A. Edelstein, P.B. Roemer, Susceptibility, lineshape, and shimming in high-resolution NMR, J. Magn. Reson. 100 (1992) 229–242.
[18] T.L. Peck, R.L. Magin, P.C. Lauterbur, Design and analysis of microcoils for NMR microscopy, J. Magn. Reson. 108B (1995) 114–124.